FOLIA HISTOCHEMICA ET CYTOBIOLOGICA
Vol. 54, No. 1, 2016
pp. 14–24

ORIGINAL PAPER

VIA MEDICA

Gene expression profiling of human bone marrow-derived mesenchymal stem cells during adipogenesis

Xiaoyuan Xu[1], Xingnuan Li[1], Ruiqiao Yan[2], He Jiang[1], Tao Wang[1], Lili Fan[1], Jianfang Wu[1], Jun Cao[1], Weidong Li[1]

[1]Key Laboratory of System Bio-medicine of Jiangxi Province, Jiujiang University, Jiujiang, PR China
[2]Clinical Skills Center, Clinic Medical College, Jiujiang University, Jiujiang, PR China

Abstract

Introduction. Adipogenesis comprises multiple processes by which mesenchymal stem cells differentiate into adipocytes. To increase our knowledge of the mechanism underlying adipogenic differentiation of human bone marrow mesenchymal stem cells (hMSCs), we performed full-genome gene expression microarray and gene ontology analyses of induced differentiation of hMSCs.

Material and methods. Adipogenic differentiation of hMSCs was induced by an adipogenic medium, and total RNA was extracted from undifferentiated hMSCs (day 0) and differentiated adipocytes (day 14). Then microarray hybridization of RNA samples was performed. The GeneChip Operating Software was used to analyze the hybridization data to identify differentially expressed genes, which were performed Gene Ontology categorization and pathway analysis. Pathway-act-network and genes-act-network were built according to the Kyoto Encyclopedia of Genes and Genomes database. Some differentially expressed genes were subjected to qRT-PCR to verify the microarray data.

Results. We detected a total of 3,821 differentially expressed genes, of which 753 were upregulated and 3,068 downregulated. These genes were well represented in a variety of functional categories, including collagen fibril organization, brown fat cell differentiation, cell division, and S phase of mitotic cell cycle. Subsequently, pathway analysis was conducted, and significant pathways (from top 50) were selected for pathway-act-network analysis, which indicated that the mitogen-activated protein kinase (MAPK) pathway and cell cycle were of high degrees (> 10). Gene-act-network analysis showed that insulin-like growth factor 1 receptor (IGF1R), histone deacetylase 1 (HDAC1), HDAC2, MAPK13, MAPK8, phosphoinositide-3-kinase regulatory subunit 1 (PI3KR1), and PI3KR2 also had high degrees (> 18).

Conclusions. Collectively, these data provide novel information and could serve as a basis for future study to clarify the mechanisms underlying adipocyte differentiation of hMSCs. *(Folia Histochem Cytobiol. 2016, Vol. 54, No. 1, 14–24)*

Key words: human bone marrow mesenchymal stem cells; adipogenic differentiation; gene microarray; pathway analysis; qRT-PCR

Introduction

Human mesenchymal stem cells (hMSCs) from bone marrow aspirates have the capacity to undergo self-renewal and multipotential differentiation [1]. *In vitro* studies have shown that MSCs can differentiate into several cell types, including adipocytes [2], chondrocytes [3], osteoblasts [4], and ligament cells [5]. When induced in a defined adipogenic medium, most hMSCs differentiate into adipocytes. Therefore, culture-expanded hMSCs would be an ideal model for the exploration of molecular events that trigger human adipogenesis [6].

In recent years, microarray assays of mRNAs have been used to follow adipogenic differentiation of preadipocytic cell lines and hMSCs [7–10]. These studies mainly focused on the hierarchical cluster analysis of adipogenic gene expression profiles,

Correspondence address: Prof. W. Li
Key Laboratory of System Bio-medicine of Jiangxi Province
Jiujiang University
Jiujiang 332000, PR China
e-mail: liweidong@outlook.com

which allows the rapid detection of alterations in the levels of gene expression as well as identification of critical genes. However, our understanding of Gene Ontology (GO) categories, pathway analysis, and pathway (gene)-act-network of hMSCs adipogenic differentiation is limited, particularly with regard to act-network analysis.

To obtain more detailed insights into human adipogenesis, we conducted gene expression profiling of human bone marrow-derived mesenchymal stem cells during adipogenesis by using microarray and bioinformatics analyses. The findings of these techniques provide new clues for future study to clarify the mechanisms of adipogenic differentiation of hMSCs.

Material and methods

Isolation and expansion of human mesenchymal stem cells. After obtaining informed consent, hMSCs were isolated from bone marrow aspirates collected from the iliac crest of a donor undergoing spinal fusion. Briefly, 5 mL of fresh bone marrow was transferred into a 5 mL of phosphate buffer solution (pH = 7.3) containing heparin (Gibco, Grand Island, NY, USA) to prevent coagulation. Adipose tissue was removed by centrifugation at 1,800 rpm for 5 min at room temperature. The hMSCs were then isolated by gradient centrifugation [8] and expanded in the medium consisting of MEM-alpha (Gibco) supplemented with 1% penicillin-streptomycin (Gibco) and 10% fetal bovine serum (Gibco). The culture medium was changed every 3–4 days, and cells were cultured at 37°C in 5% CO_2 and passaged upon reaching 80% confluency. The Ethics Committee of the Medical Faculty at Jiujiang University approved the collection of bone marrow from the donor.

Flow cytometry analysis. To verify isolation and enrichment of hMSCs, cells in passage 4 were incubated with fluorescein-isothiocyanate (FITC) anti-human CD34 antibody (Ab), FITC anti-human CD44 Ab, FITC anti-human CD45 Ab, FITC anti-IgG1, PE anti-human CD19 Ab, PE anti-human CD90 Ab, PE anti-human CD105 Ab and PE anti-IgG1(all purchased from Biolegend, San Diego, CA, USA) for 1 h at 4°C. All samples were tested and analyzed with a FACSCalibur system (Becton Dickinson, San Jose, CA, USA).

Adipogenic differentiation. Adipogenic differentiation was performed according to the method described elsewhere, with minor modifications [9–10]. The hMSCs were seeded at a density of 10^4 cells/cm^2 before induction. Upon reaching confluency, the hMSCs were stimulated in an adipogenic medium composed of MEM-alpha with 10% FBS, 100 μg/mL indomethacin, 1 μM dexamethasone, 0.5 mM 3-isobutyl-1--methyl-xanthine and 0.01 mg/mL insulin for 14 days (all purchased from Sigma, St. Louis, Mo, USA).

Oil red O staining. The cells were rinsed with PBS (500 μL) and fixed with 10% neutral buffered formalin (500 μL). The cells were then washed with 60% 2-propanol (500 μL) for 2–5 min and stained with oil red O (500 μL) for 5 min after washing with sterile water. The cells were rinsed with water and stained with Harris' hematoxylin (500 μL) for 1 min, then rinsed with water. Lipid vesicles were observed under an IX71 Olympus microscope (Olympus, Tokyo, Japan).

RNA preparation. Total RNA was extracted from undifferentiated hMSCs (day 0) and differentiated adipocytes (day 14) using the TRIzol® reagent, according to the manufacturer's instructions (Invitrogen, Carlsbad, CA, USA). Then, RNA was purified using the NucleoSpin RNA clean-up kit (Macherey-Nagel, Düren, Germany). RNA quality was determined by formaldehyde denaturation electrophoresis and only those samples that exhibited no degradation (ratios approaching 2:1 for the 28S to 18S bands) were used in subsequent analyses. RNA concentration was assessed by using a Nanodrop 2000 spectrophotometer (Thermo, Wilmington, DE, USA).

Microarray hybridization and data analysis. The RNA samples were sent to CapitalBio Corporation (Beijing, China) for microarray hybridization. Briefly, double-stranded cDNA was synthesized from total RNA using a T7-oligo (dT) primer. The cDNA was purified and further converted into cRNA using an *in vitro* transcription reaction. Approximately 5 μg of cRNA was reverse-transcribed to cDNA and then labeled with Cy3-dCTP using a Klenow enzyme. The labeled cDNA fragments were then hybridized to NimbleGen Human Genome Expression Arrays for 16 h at 42°C using the Roche NimbleGen Hybridization System 12 (Roche NimbleGen, Madison, WI, USA). Afterwards, the gene chips were washed, and then scanned in a LuxScan 10KA system (CapitalBio, Beijing, China). Images were transformed into digital data using LuxScan 3.0 image analysis software (CapitalBio). Microarray data were normalized by LOWESS normalization of each array using the R package.

The GeneChip Operating Software (GCOS 1.4) was used to analyze the hybridization data. The scanned images were first assessed by visual inspection, then analyzed to generate raw data files saved as CEL files using the default setting of GCOS 1.4. Robust Multichip Analysis (RMA) was used to normalize the different arrays. Linear models and empirical Bayes methods were used to identify differentially expressed genes [11]. The Benjamini Hochberg (BH) false discovery rate (FDR) algorithm was used to adjust the resulting *P* values [12]. Differential expression of genes was considered to be significant only when the FDR values were < 0.05 (controlling the expected FDR to no more than 5%), as well as the fold change (FC) was $\geq |1.5|$.

Analysis of GO category, pathway, pathway (gene)-act-network. Differentially expressed genes were determined from

Table 1. Primers used in this study

Gene symbol	Forward primers	Reverse primers	Length (bp)
FABP4	5'-CATGGCCAAACCTAACATGA-3'	5'-CAAATTCCTGGCCCAGTATG-3'	110
ADIPOQ	5'-CCTAAGGGAGACATCGGTGA-3'	5'-CAATCCCACACTGAATGCTG-3'	132
PPARγ	5'-CGAGAAGGAGAAGCTGTTGG-3'	5'-TCAGCGGGAAGGACTTTATG-3'	122
ZBTB16	5'-AAGCGGTTCCTGGATAGTTT-3'	5'-ATGTCAGTGCCAGTATGGGT-3'	149
SFRP1	5'-GACTCGTGCGAGCCGGTCAT-3'	5'-TTGGAGGCTTCGGTGGCATT-3'	125
SFRP2	5'-GCCACCCGGACACCAAGAAG-3'	5'-GGGAAGCCGAAGGCGGACAT-3'	147
LEPR	5'-GAATGCATTTTCCAGCCAAT-3'	5'-TGGCTTCACCACAGAATCAG-3'	123
IGF1	5'-GAAGGTGAAGATGCACACCA-3'	5'-CACGAACTGAAGAGCATCCA-3'	138
IGFBP2	5'-GAGAAGGTCACTGAGCAGCA-3'	5'-ACCTGGTCCAGTTCCTGTTG-3'	125
FRZB	5'-TCTGCACCATTGACTTCCAG-3'	5'-GTCGTACACTGGCAGCTCCT-3'	146
PIK3R1	5'-TGGTGGACGGCGAAGTAAAG-3'	5'-TTGAGGGAGTCGTTGTGCTG-3'	148
IGFBP6	5'-GAATCCAGGCACCTCTACCA-3'	5'-TGGGCACGTAGAGTGTTTGA-3'	149
MYEF2	5'-TGGAATGGGTAGCATGAACA-3'	5'-CGATCCATATCGATGCTCCT-3'	126
MAPK13	5'-CCCTCACCCATCCCTTCTTT-3'	5'-ATGTGCTGCTTCCATTCATC-3'	121
FGF2	5'-CCACTTCAAGGACCCCAAG-3'	5'-CTTGATGTGAGGGTCGCTCT-3'	114
FGF5	5'-TTCTTCAGCCACCTGATCCT-3'	5'-CGCTACTGCTGCTCTGTCTG-3'	130
GNB5	5'-GGAGGTTGCCATCTATTCCA-3'	5'-CCCTTTGAGAACATCCCAGA-3'	131
VEGFA	5'-CGCAAGAAATCCCGGTATAA-3'	5'-AAATGCTTTCTCCGCTCTGA-3'	119
NR3C1	5'-GGCAATACCAGGTTTCAGGA-3'	5'-ACACAGCAGGTTTGCACTTG-3'	131

Details of gene symbols are presented in Table 4 and Table S1 of Supplementary data

statistical outcomes by testing for association with biological process GO terms. The GO category was classified using Fisher's exact test, and FDR was calculated to correct the *P* value, because the smaller the FDR, the smaller the error in judging the *P* value [13].

Pathway analysis was used to identify the significant pathway of the differentially expressed genes according to KEGG (Kyoto Encyclopedia of Genes and Genomes). Similarly, Fisher's exact test, followed by BH multiple testing correction, was performed to select the significant pathway, and the threshold of significance was defined by *P* value and FDR [14–15].

The KEGG database was used to build the network of pathways based on the relationship between the pathways and compounds in the database [16–18]. Similarly, the differentially expressed genes were selected to build genes-act-network according to the relationship among the genes, proteins, and compounds in the KEGG database.

Degree centrality is defined as the number of links of each node to another in the pathway(gene)-act-network. Outdegree pertains to the number of pathways (upstream) acting on another pathway (downstream). Indegree indicates the number of pathways (downstream) acted on by another pathway (upstream). Outdegree may also pertain to the number of genes acted on by a specific gene, and indegree shows the number of genes acting on a specific gene.

Quantitative real-time PCR (qRT-PCR) analysis. qRT-PCR was used to validate selected microarray data. Total RNA was reverse-transcribed using the PrimeScript RT reagent Kit (Takara, Tokyo, Japan) according to the manufacturer's instructions, with GAPDH as endogenous control. The genes and primers used in qRT-PCR analysis are listed in Table 1. The cDNA samples were used for qRT-PCR analysis, which was performed using a 7300 Real-Time PCR System (ABI, Foster, CA, USA) with SYBR Premix Ex TaqTM (Takara), following the manufacturer's instructions. Each sample was run in triplicate. Relative fold-change was calculated according to the $2^{-\Delta\Delta^{CT}}$ method.

Results

Surface marker presentation of hMSCs

hMSCs were isolated from bone marrow aspirates and expanded in culture media. To verify cell identity, the cultured cells were routinely investigated by flow cytometry analysis at the 4th passage. Measurements revealed a uniformly positive cell population that

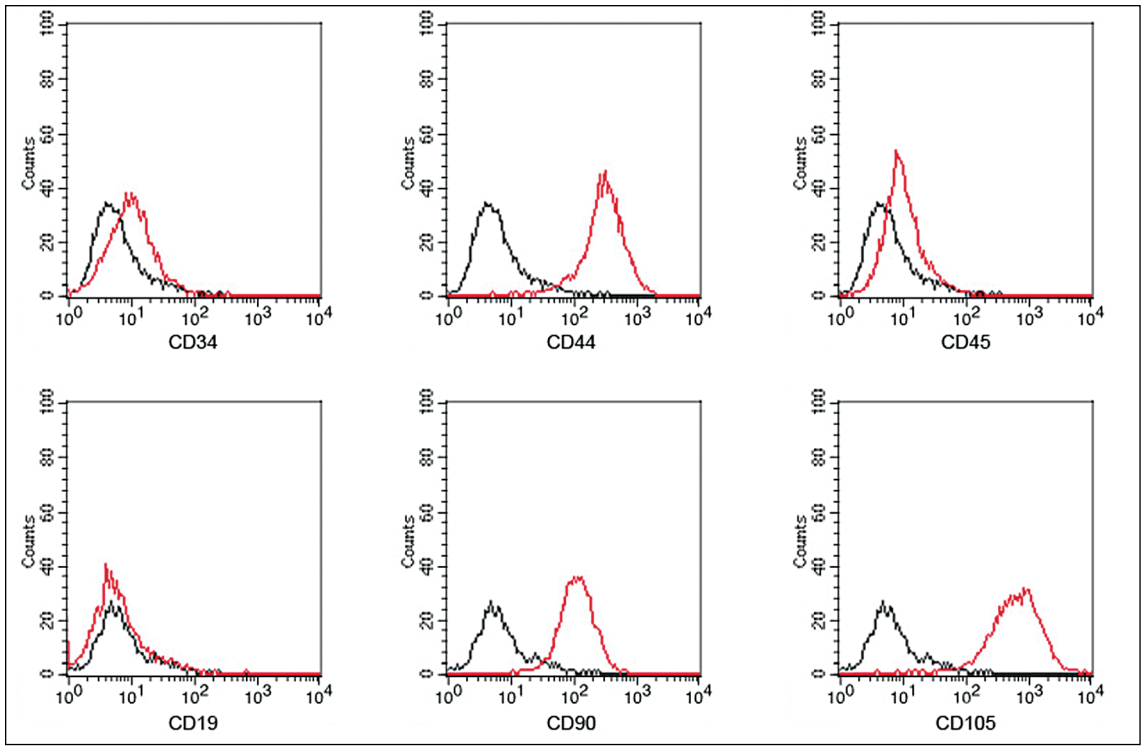

Figure 1. Surface marker presentation of human bone marrow mesenchymal stem cells (hMSCs). hMSCs were positive for reactivity to antigens CD44, CD90, and CD105, and negative for reactivity to antigens CD19, CD34, and CD45 (red lines); black lines represent IgG1 isotypic control

expressed CD44, CD90, and CD105 but did not express CD19, CD34, and CD45 (Figure 1).

Adipogenesis of hMSCs

In response to the administration of adipogenic medium, adipogenesis of hMSCs was identified at day 14. The majority of the cells accumulated lipid vesicles in the cytoplasm, which was positively stained with oil red O (Figure 2), whereas cells were heterogeneous in the degree of staining.

Microarray analysis

To explore the adipogenic differentiation of hMSCs, we performed differential gene expression profiling utilizing full-genome gene expression microarrays. Upregulation of a gene was defined as a FC in relative transcription levels of Log FC > 1 and FDR < 0.05. On the other hand, downregulation of a gene was defined as Log FC < –1 and FDR < 0.05. Genes with relative transcription levels of –1 < Log FC < 1 were considered to present no notable changes. In the present study, the adipogenesis of hMSCs contributed to the differential expression of 3,821 genes (Supplementary data: Table S1).

Gene Ontology (GO) categorization

The 3,821 differentially expressed genes were classified into different functional categories according to the GO project for biological process; among these, 753 genes were upregulated and 3,068 genes were downregulated. The primary GO categories for upregulated genes were collagen fibril organization, brown fat cell differentiation, and positive regulation of fat cell differentiation (Figure 3A). The main GO categories for downregulated genes were cell cycle, S phase of mitotic cell cycle, and G1/S transition of mitotic cell cycle (Figure 3B).

Pathway analysis

Pathway analysis was conducted to identify the significant pathways (from the top 50) of the differentially expressed gene sets according to KEGG. Through a selection process, the upregulated genes were determined to be mainly involved in the PPAR (peroxisome proliferator-activated receptor), adipocytokine, and Wnt signaling pathways (Figure 4A). The downregulated genes were mainly involved in the cell cycle, axon guidance, and Jak-STAT signaling pathway (Figure 4B).

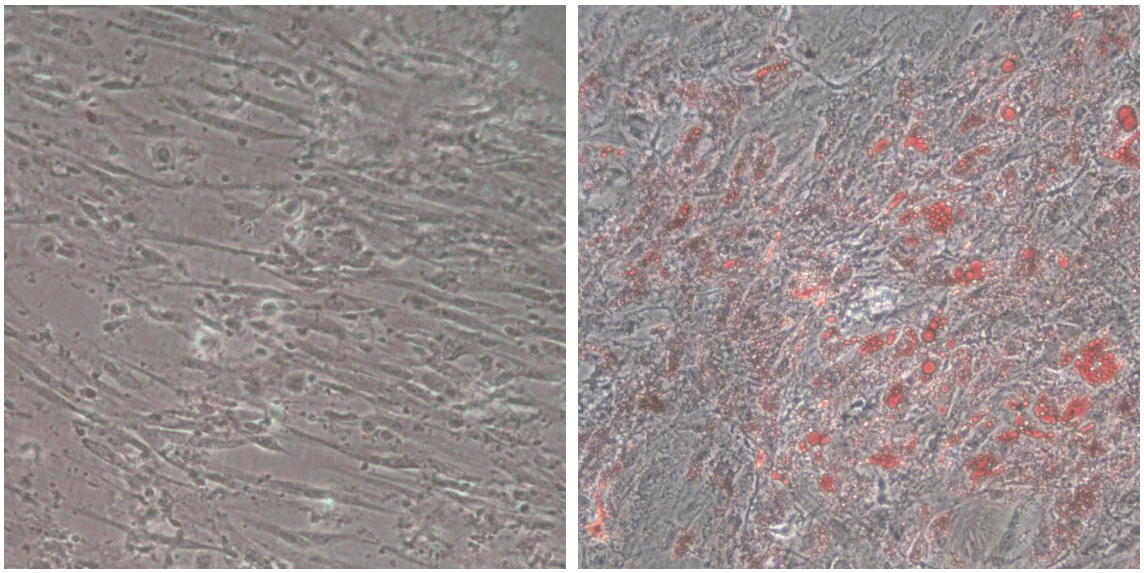

Figure 2. Adipogenesis of human bone marrow mesenchymal stem cells (hMSCs). hMSCs were cultured in an adipogenic medium. Oil-red O staining of lipid-droplets at day 14 confirmed adipogenesis (×20)

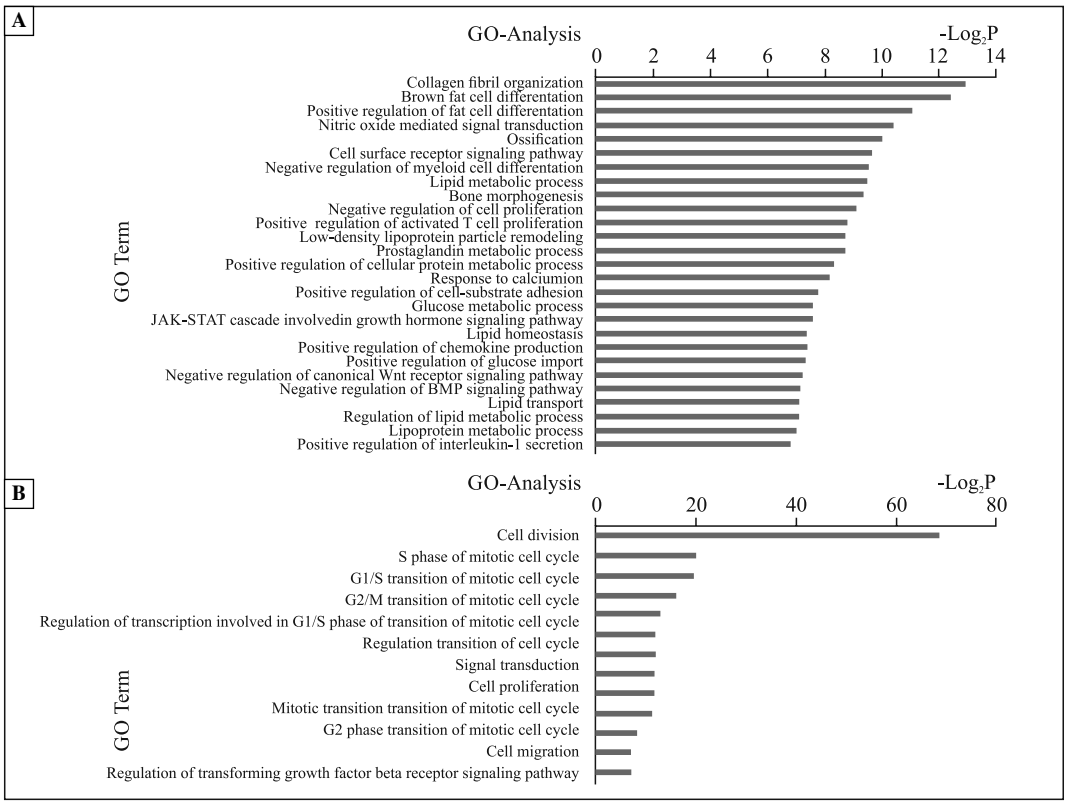

Figure 3. Gene Ontology (GO) category based on biological process for differentially expressed genes. **A.** The significant GO categories for upregulated genes; **B.** The significant GO categories for downregulated genes. *P*-value < 0.05 and false discovery rate < 0.05 were used as threshold for the selection of significant GO categories

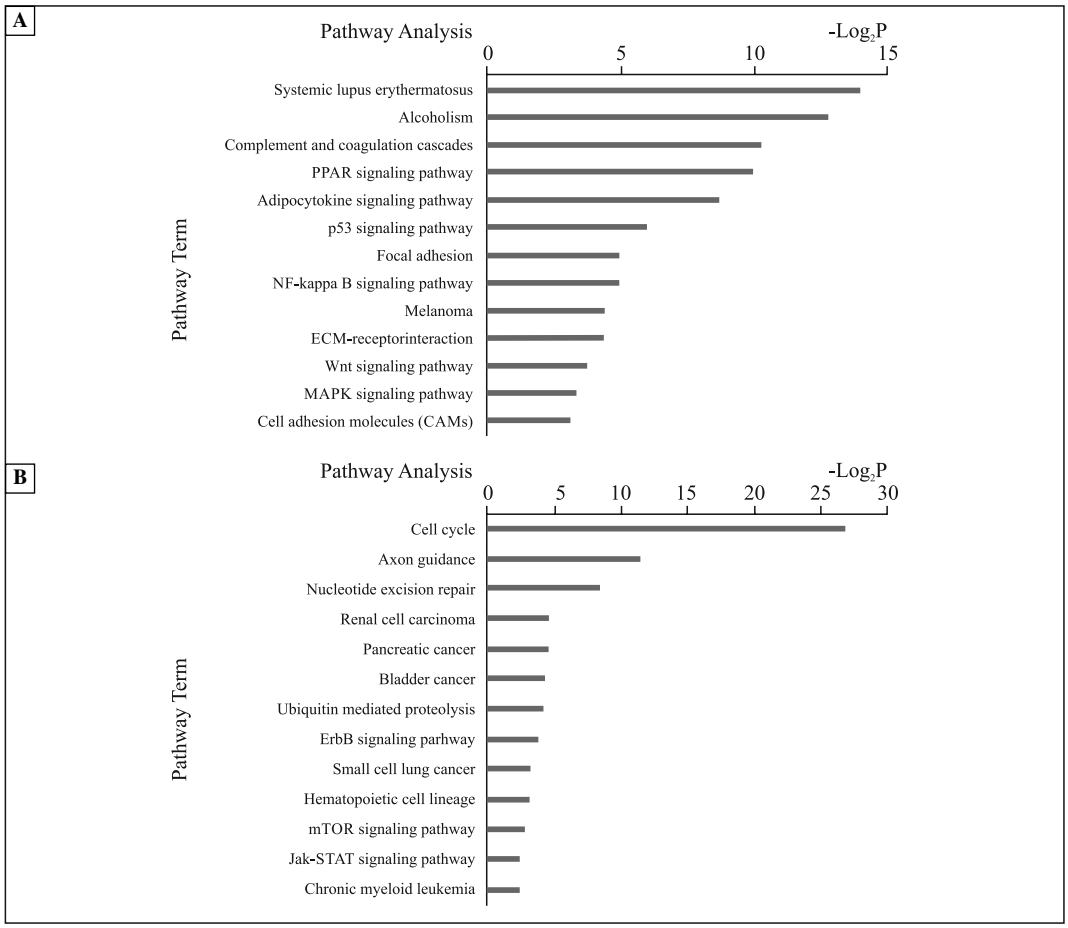

Figure 4. Kyoto Encyclopedia Genes and Genomes (KEGG) pathway analysis of differentially expressed genes. **A.** The significant pathways of upregulated genes; **B.** The significant pathways of downregulated genes. *P*-value < 0.05 and false discovery rate < 0.05 were used as threshold for the selection of significant KEGG pathways

Pathway-act-network

To illustrate the identified pathway terms, we built the pathway-act-network according to the relationship between the differential pathways using the KEGG database (Figure 5). In this network of pathway interaction, the MAPK signaling pathway and cell cycle may be the most important pathways because these showed the strongest degree of centrality (Table 2).

Gene-act-network

The construction of a gene-act-network was similar to that of the pathway-act-network (Figure 6). The genes in the gene network were also involved in the significant pathway (from the top 50), and the node point was the "gene", instead of the "pathway" (Table 3).

Confirmation of gene expression by qRT-PCR analysis

To verify the data obtained by microarray analysis, qRT-PCR was performed on 19 differentially expressed genes (11 upregulated and 8 downregulated). These genes also included the adipogenic marker genes (FABP4, ADIPOQ, and PPARG). A high correlation was observed between the qRT-PCR and microarray data. The detected FC in expression is shown in Table 4.

Discussion

Adipogenic differentiation of hMSCs is a complex process that requires the precise regulation of cellular interactions with multiple differentiation factors and components of the extracellular matrix [19]. Therefore, various signaling pathways, adhesion molecules, and transcription factors play important roles in this process [20]. Because the applied cocktail of adipogenic inducers promotes the differentiation of hMSCs into adipocytes [8–10], these MSCs were further used for gene expression profiling during adipogenesis [1].

In the present study, a total of 3,821 adipogenic candidate genes, of which 753 were upregulated and

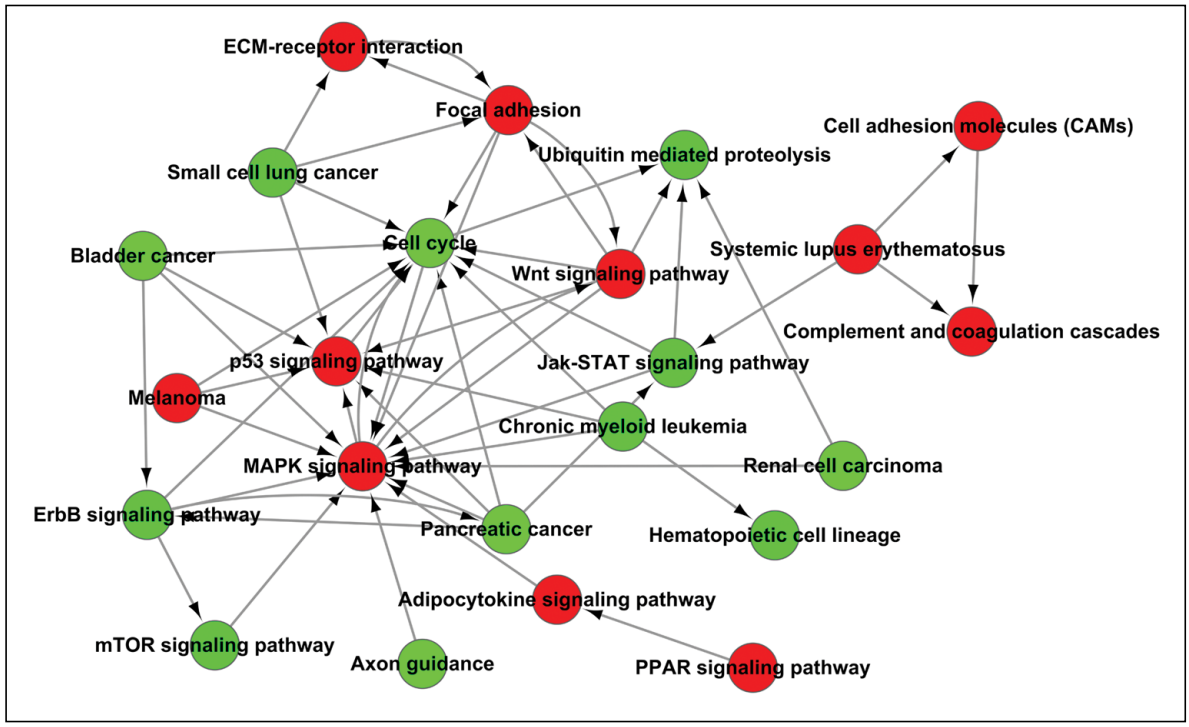

Figure 5. Pathway-act-network according to the relationship between the differential pathways. Each research unit (node point) shown as a circle represents a significant pathway. Each network node point was labeled according to the node relative position (downstream or upstream) in the network graph. A node point acts on another node as indicated by arrows, which represent the direction from the upstream pathway to the downstream pathway. The red node indicates the pathway of the upregulated genes, and the green node represents the pathway for the downregulated genes

Table 2. The degree of involved partial pathways in the pathway-act-network

Pathway	Indegree	Outdegree	Degree
MAPK signaling pathway	13	3	16
Cell cycle	11	2	13
p53 signaling pathway	7	1	8
Focal adhesion	3	4	7
Wnt signaling pathway	2	5	7
ErbB signaling pathway	2	4	6
Jak-STAT signaling pathway	2	3	5
Ubiquitin mediated proteolysis	4	0	4
ECM-receptor interaction	2	1	3
mTOR signaling pathway	1	1	2
Adipocytokine signaling pathway	1	1	2
Cell adhesion molecules	1	1	2
PPAR signaling pathway	0	1	1

Interactions and functional network identified by Kyoto Encyclopedia of Genes and Genomes analysis. Degree centrality is defined as the number of links that one node has to another. Outdegree — the number of pathways (upstream) that act on a specific pathway (downstream); indegree — the number of pathways (downstream) that are acted on by a specific pathway (upstream)

3,068 were downregulated, were differentially expressed during adipogenic development of hMSCs. The identified upregulated and downregulated genes detected during adipogenic differentiation were then used in GO category analysis. Our results indicated that these differentially expressed genes belonged to a variety of functional categories (Figures 3A and 3B). Here, we mainly focused on some GO categories closely related to adipogenic differentiation. The upregulated genes, for example, were associated with collagen fibril organization, brown fat cell differentiation, positive regulation of fat cell differentiation, and cell surface receptor signaling pathway. Downregulated genes were associated with cell division, S phase of mitotic G1/S transition of mitotic cell cycle, and G2/M transition of the mitotic cell cycle. We also determined that the genes involved in cell differentiation were upregulated, whereas genes involved in cell division and cell cycle were downregulated. GO analysis showed that cell differentiation was the predominant biological activity compared to cell division or cell cycle, thus confirming the findings of previous studies [21–23].

GO analysis involves various genes with different functions and features [24, 25]. In the present study, we determined that some differentially expressed

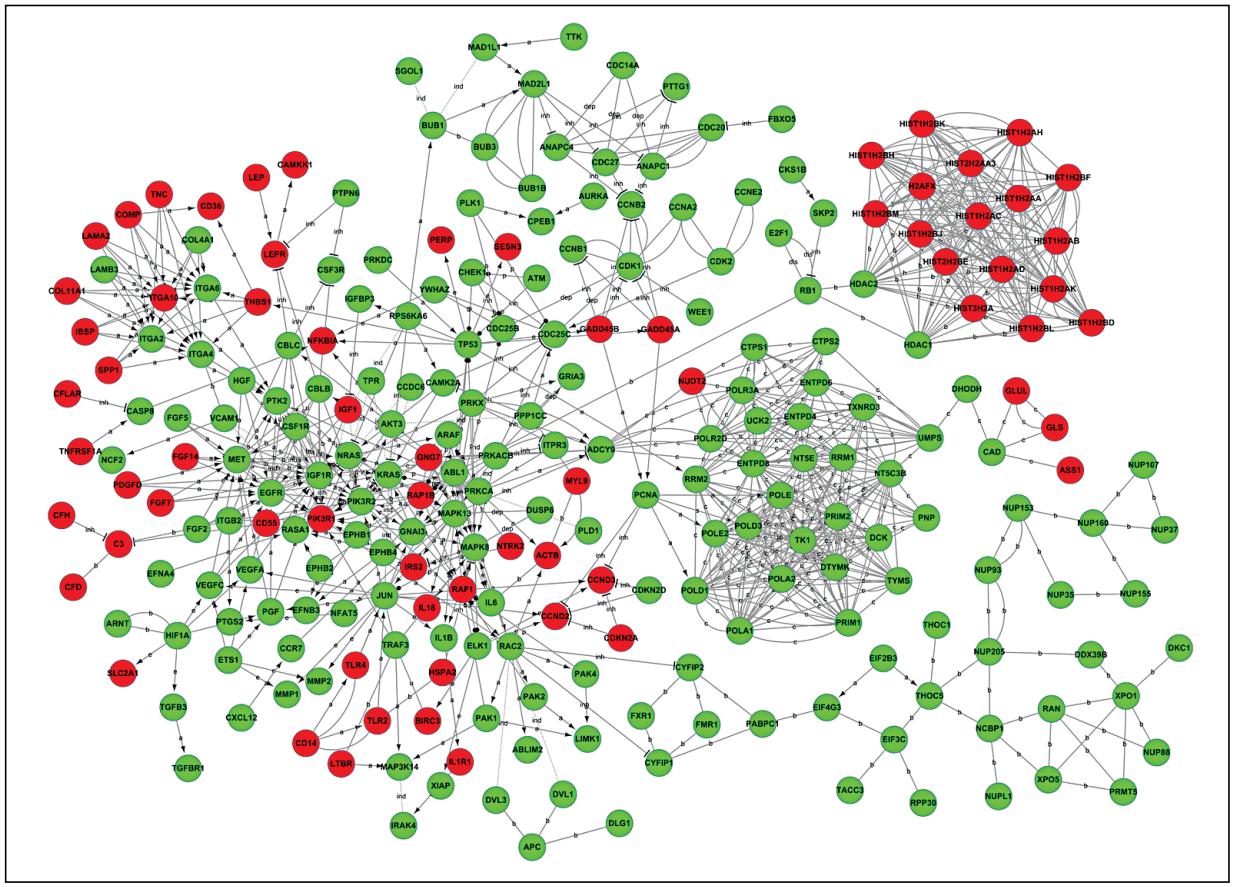

Figure 6. Gene-act-network according to the relationship among the differentially expressed genes. Genes in red and green indicate upregulated and downregulated expressed genes, respectively. The regulation relationships of different genes are described with terms such as "indirect effect (ind), inhibition (inh), dephosphorylation (dep), activation (a), binding (b), and compound (c)"

Table 3. The degree of involved partial genes in the gene--act-network

Gene	Indegree	Outdegree	Degree
IGFR1	15	11	26
PI3KR1	16	5	21
PI3KR2	16	5	21
HDAC1	0	18	18
HDAC2	0	18	18
MAPK8	12	7	19
MAPK13	9	9	18

Interactions and functional network identified by Kyoto Encyclopedia of Genes and Genomes. Degree centrality is defined as the number of links that one node has to another. Indegree — the number of genes acting on a specific gene; outdegree — the number of genes acted on by a specific gene

genes were involved in various GO terms that have not yet been described in the context of adipogenesis, such as the zinc finger, the BTB domain-containing protein 16 (ZBTB16), secreted frizzled-related protein 1 (SFRP1), and SFRP2. For example, ZBTB16 was first identified in acute promyelocytic leukemia, being also expressed in the perinatal kidney, heart, and liver and during the development of limb buds and the central nervous system [26]. Some findings have already confirmed that ZBTB16 is an upstream regulator of CBFA1 (Core-binding factor 1) and plays an important role in osteoblastic differentiation [27], although little is known about its role in adipogenic differentiation. In our study, ZBTB16 was highly upregulated and was linked to several significant GO terms, thereby indicating that it plays an important role and may be a new candidate gene in adipogenic differentiation of hMSCs. Therefore, GO analysis can provide novel information which may facilitate selection of genes for more in-depth analysis in relation to adipogenic differentiation.

Pathway analysis is a systematic description of various biomolecular and signaling molecules that interact and regulate each other. The KEGG database facilitates identification of pathways of differentially

Table 4. Verification of gene expression changes by qRT-PCR

Gene symbol	Description	Fold-change of expression (log_2FC)	
		Microarray	qRT-PCR
FABP4	Fatty acid binding protein 4, adipocyte	5.9	7.0
ADIPOQ	Adiponectin, C1Q and collagen domain containing	1.6	3.2
PPARG	Peroxisome proliferator-activated receptor gamma	5.0	3.5
ZBTB16	Zinc finger and BTB domain containing 16	4.3	3.1
SFRP1	Secreted frizzled-related protein 1	4.6	3.8
SFRP2	Secreted frizzled-related protein 2	1.5	2.6
LEPR	Leptin receptor	3.2	4.7
IGF1	Insulin-like growth factor 1 (somatomedin C)	3.6	5.4
IGFBP2	Insulin-like growth factor binding protein 2, 36 kDa	4.2	4.9
FRZB	Frizzled-related protein	4.6	3.9
PIK3R1	Phosphoinositide-3-kinase, regulatory subunit 1 (alpha)	1.6	1.9
IGFBP6	Insulin-like growth factor binding protein 6	–3.0	–2.1
MYEF2	Myelin expression factor 2	–2.4	–2.0
MAPK13	Mitogen-activated protein kinase 13	–1.8	–3.1
FGF2	Fibroblast growth factor 2 (basic)	–1.9	–2.8
FGF5	Fibroblast growth factor 5	–1.4	–1.7
GNB5	Guanine nucleotide binding protein (G protein), beta 5	–1.4	–1.6
VEGFA	Vascular endothelial growth factor A	–3.2	–1.9
NR3C1	Nuclear receptor subfamily 3, group C, member 1 (glucocorticoid receptor)	–1.4	–2.0

expressed genes (Figures 4A and 4B). Because the PPARg signaling pathway and the adipocytokine signaling pathway have been extensively studied [28], we selected other pathways closely related to adipogenic differentiation for analysis in the present study.

The MAPK signaling pathway is one of the most actively studied areas in cellular signal transduction, and recent studies have shown that it plays an important regulatory role during human adipogenic differentiation [29]. In the present study, genes related to this pathway included dual specificity phosphatase 14 (DUSP14), neurotrophin 3 (NTF3), fibroblast growth factor 14 (FGF14), FGF7, and CD14 molecule. Fibroblast growth factors (FGFs) play an important major role in the control of cell proliferation and differentiation [30, 31]. A recent study demonstrated that FGF7 promotes preadipocyte proliferation [32]. In addition, FGF2 also induces cell growth and chondrogenic and osteoblast differentiation in bone marrow-derived mesenchymal cells [33, 34]. However, the role of FGFs in adipogenic differentiation of hMSCs, especially FGF7 and FGF14, remains elusive. The results of the present study suggest that FGF7 and FGF14 regulate adipogenic differentiation of hMSCs *via* the MAPK pathway.

In addition, cell division (pathway) pertains to a series of events that occur in a cell leading to its division and duplication. Our results showed that 53 genes, including E2F transcription factor 1 (E2F1), polo-like kinase 1 (PLK1), cyclin B2 (CCNB2), and cyclin-dependent kinase 2 (CDK2), are involved in this particular pathway. These results suggest that these cell cycle-related genes should be further studied in relation to adipogenic differentiation.

To further explore the relationship among these pathways, we performed pathway-act-network analysis based on the results of pathway analysis. In systems biology, a pathway is composed of a variety of genes and its proteins and usually is not independent on cells. Thus, there are interactive contacts (crosstalk) among different pathways, thereby forming an organic network regulation. We can intuitively depict the important relationships among significant pathways using network diagrams.

In the present study, we determined that the significant pathways for upregulated genes mainly consisted of the MAPK, Wnt, and P53 signaling pathways. On the other hand, the significant pathways for downregulated genes mainly comprised the cell cycle, bladder

cancer, and Jak-STAT signaling pathways (Figure 5). Based on these findings, we mainly analyzed the different statistical values of degree (Table 2). The MAPK pathway and cell cycle (as downstream pathways) showed high indegree (> 10), indicating that these were the end points of signal transmission during the adipogenic differentiation of hMSCs. There were also upstream pathways that acted on other downstream pathways. These findings indicated that these two pathways were the most important and critical measures for the centrality of a pathway, which in turn determines its relative importance within a network [35].

The most notable function of the PPARγ signaling pathway is to regulate the development of adipose tissues, which involves the coordinated expression of several genes that are responsible for adipogenic differentiation [36]. In the present study, the degree value of the PPARγ signaling pathway is 1, indicating that it was one of the initiators of the whole network. Taken together, this is the first attempt to illustrate the action and relationship among various pathways by using a pathway-act-network.

Subsequently, a gene-act-network was constructed (Figure 6 and Table 3). A gene can participate in several pathways, and various kinds of genes are related to each other. Therefore, a gene-act-network can precisely respond to this regulated type of relationship. Similarly to the pathway-act-network, we also found some genes such as the insulin-like growth factor 1 receptor (IGF1R), HDAC1, HDAC2, mitogen-activated protein kinase 13 (MAPK13), MAPK8, phosphoinositide-3-kinase regulatory subunit 1 alpha (PI3KR1), and phosphoinositide-3-kinase regulatory subunit 2 beta (PI3KR2), which are closely related to cell proliferation and differentiation [37–40]. In light of our findings and those of previous reports, we have determined that earlier investigations on the differentiation of hMSCs to adipocytes did not provide satisfactory results, particularly relating to IGF1R and HDACs. In our study these genes showed relatively high degree values, which was indicative of dense and complex regulatory networks (Table 3). Similarly, the degree centrality represents the key and important measures of the centrality of a gene within a network. By conducting gene-act-network analysis, we have discovered not only the signaling transduction but also the key regulatory genes associated with the adipogenic differentiation of hMSCs.

In conclusion, we applied microarray and bioinformatics technology and exhibited gene expression profiling during adipogenesis in human bone marrow-derived mesenchymal stem cells. These data provide novel information and could serve as a basis for future studies on elucidating the mechanism underlying adipogenic differentiation of hMSCs.

Acknowledgments

The authors wish to thank Drs. Dai Chen and Bo Zhang (Novel Bioinformatics Ltd., Co, Shanghai, China) for their technical assistance in bioinformatics analysis. The National Natural Science Foundation of China (Nos. 81160113 and 81460221) supported this study.

References

1. Pittenger MF, Mackay AM, Beck SC et al. Multilineage potential of adult human mesenchymal stem cells. *Science*. 1999;284:143–147. doi: 10.1126/science.284.5411.143.
2. Helder MN, Knippenberg M, Klein-Nulend J et al. Stem cells from adipose tissue allow challenging new concepts for regenerative medicine. *Tissue Eng*. 2007;13:1799–1808. doi: 10.1089/ten.2006.0165.
3. Barry F, Boynton RE, Liu B et al. Chondrogenic differentiation of mesenchymal stem cells from bone marrow: differentiation-dependent gene expression of matrix components. *Exp Cell Res*. 2001;268:189–200. doi: 10.1006/excr.2001.5278.
4. Arinzeh TL. Mesenchymal stem cells for bone repair: preclinical studies and potential orthopedic applications. *Foot Ankle Clin*. 2005;10:651–665. doi: 10.1016/j.fcl.2005.06.004.
5. Hankemeier S, van Griensven M, Ezechieli M et al. Tissue engineering of tendons and ligaments by human bone marrow stromal cells in a liquid fibrin matrix in immunodeficient rats: results of a histologic study. *Arch Orthop Traum. Surg*. 2007;127:815–821. doi: 10.1007/s00402-007-0366-z.
6. Subash-Babu P, Alshatwi AA. Aloe-emodin inhibits adipocyte differentiation and maturation during in vitro human mesenchymal stem cell adipogenesis. *J Biochem Mol Toxicol*. 2012;26:291–300. doi: 10.1002/jbt.21415.
7. Burton GR, Nagarajan R, Peterson CA et al. Microarray analysis of differentiation-specific gene expression during 3T3-L1 adipogenesis. *Gene*. 2004;329:167–185. doi: 10.1016/j.gene.2003.12.012.
8. Sekiya I, Larson BL, Vuoristo JT et al. Adipogenic differentiation of human adult stem cells from bone marrow stroma (MSCs). *J Bone Miner Res*. 2004;19:256–264. doi: 10.1359/JBMR.0301220.
9. Menssen A, Häupl T, Sittinger M et al. Differential gene expression profiling of human bone marrow-derived mesenchymal stem cells during adipogenic development. *BMC Genomics*. 2011;12:461. doi: 10.1186/1471-2164-12-461.
10. Nakamura T, Shiojima S, Hirai Y et al. Temporal gene expression changes during adipogenesis in human mesenchymal stem cells. *Biochem Biophys Res Commun*. 2003;303:306–312. doi: 10.1016/S0006-291X(03)00325-5.
11. Smyth GK. Linear models and empirical bayes methods for assessing differential expression in microarray experiments. *Stat Appl Genet Mol Biol*.2004;3:1–25. doi: 10.2202/1544-6115.1027.
12. Benjamini Y, Hochberg Y. Controlling the false discovery rate: a practical and powerful approach to multiple testing. *J R Stat Soc Series B Stat Methodol*. 1995;57:289–300.
13. Dupuy D, Bertin N, Hidalgo CA et al. Genome-scale analysis of in vivo spatiotemporal promoter activity in Caenorhabditis elegans. *Nat Biotechnol*. 2007;25:663–668. doi: 10.1038/nbt1305.
14. Draghici S, Khatri P, Tarca AL et al. A systems biology approach for pathway level analysis. *Genome Res*. 2007;17:1537–1545. doi: 10.1101/gr.6202607.

15. Yi M, Horton JD, Cohen JC et al. Whole Pathway Scope: a comprehensive pathway-based analysis tool for high-throughput data. *BMC Bioinformatics*. 2006;7:30. doi: 10.1186/1471-2105-7-30.
16. Li C, Li H. Network-constrained regularization and variable selection for analysis of genomic data. *Bioinformatics*. 2008;24:1175–1182. doi: 10.1093/bioinformatics/btn081.
17. Prieto C, Risueno A, Fontanillo C et al. Human gene coexpression landscape: confident network derived from tissue transcriptomic profiles. *PLoS ONE*. 2008;3:e3911. doi: 10.1371/journal.pone.0003911.
18. Zhang JD, Wiemann S. KEGG graph: a graph approach to KEGG PATHWAY in R and bioconductor. *Bioinformatics*. 2009;25:1470–1471. doi: 10.1093/bioinformatics/btp167.
19. Imhoff BR, Hansen JM. Differential redox potential profiles during adipogenesis and osteogenesis. *Cell Mol Biol Lett*. 2011;16:149–161. doi: 10.2478/s11658-010-0042-0.
20. Sanz C, Vázquez P, Blázquez C et al. Signaling and biological effects of glucagon-like peptide 1 on the differentiation of mesenchymal stem cells from human bone marrow. *Am J Physiol Endocrinol Metab*. 2010;298:E634–E643. doi: 10.1152/ajpendo.00460.2009.
21. Köllmer M, Buhrman JS, Zhang Y et al. Markers are shared between adipogenic and osteogenic differentiated mesenchymal stem cells. *J Dev Biol Tissue Eng*. 2013;5:18–25. doi: 10.5897/JDBTE2013.0065.
22. Zhang Y, Khan D, Delling J et al. Mechanisms underlying the osteo-and adipo-differentiation of human mesenchymal stem cells. *Sci World J*. 2012;793823. doi: 10.1100/2012/793823.
23. Zhao YM, Li JY, Lan JP et al. Cell cycle dependent telomere regulation by telomerase in human bone marrow mesenchymal stem cells. *Biochem Biophys Res Commun*. 2008;369:1114–1119. doi: 10.1016/j.bbrc.2008.03.011.
24. Torto-Alalibo T, Meng S, Dean RA. Infection strategies of filamentous microbes described with the Gene Ontology. *Trends Microbiol*. 2009;17:320–327. doi: 10.1016/j.tim.2009.05.003.
25. Park J, Costanzo MC, Balakrishnan R et al. CvManGO, a method for leveraging computational predictions to improve literature-based Gene Ontology annotations. *Database (Oxford)*. 2012:bas001. doi: 10.1093/database/bas001.
26. Cook M, Gould A, Brand N et al. Expression of the zinc-finger gene PLZF at rhombomere boundaries in the vertebrate hindbrain. *Proc Natl Acad Sci USA*. 1995;92:2249–2253. PMID: 7892256.
27. Ikeda R, Yoshida K, Tsukahara S et al. The promyelotic leukemia zinc finger promotes osteoblastic differentiation of human mesenchymal stem cells as an upstream regulator of CBFA1. *J Biol Chem*. 2005;280:8523–8530. doi: 10.1074/jbc.M409442200.
28. Yu WH, Li FG, Chen XY et al. PPARγ suppression inhibits adipogenesis but does not promote osteogenesis of human mesenchymal stem cells. *Int J Biochem Cell Biol*. 2012;44:377–384. doi: 10.1016/j.biocel.2011.11.013.
29. Wang M, Wang JJ, Li J et al. Pigment epithelium-derived factor suppresses adipogenesis via inhibition of the MAPK/ERK pathway in 3T3-L1 preadipocytes. *Am J Physiol Endocrinol Metab*. 2009;297:E1378–E1387. doi: 10.1152/ajpendo.00252.2009.
30. Marie PJ. Fibroblast growth factor signaling controlling osteoblast differentiation. *Gene*. 2003;316:23–32. doi: 10.1016/S0378-1119(03)00748-0.
31. Ornitz DM. FGF signaling in the developing endochondral skeleton. *Cytokine Growth Factor Rev*. 2005;16:205–213. doi: 10.1016/j.cytogfr.2005.02.003.
32. Zhang T, Guan H, Yang K. Keratinocyte growth factor promotes preadipocyte proliferation via an autocrine mechanism. *J Cell Biochem*. 2010;109:737–746. doi: 10.1002/jcb.22452.
33. Biver E, Soubrier AS, Thouverey C et al. Fibroblast growth factor 2 inhibits up-regulation of bone morphogenic proteins and their receptors during osteoblastic differentiation of human mesenchymal stem cells. *Biochem Biophys Res Commun*. 2012;427:737–742. doi: 10.1016/j.bbrc.2012.09.129.
34. Handorf AM, Li WJ. Fibroblast growth factor-2 primes human mesenchymal stem cells for enhanced chondrogenesis. *PLoS One*. 2011;6:e22887. doi: 10.1371/journal.pone.0022887.
35. Barabasi AL, Oltvai ZN. Network biology: understanding the cell's functional organization. *Nat Rev Genet*. 2004;5:101–113. doi: 10.1038/nrg1272.
36. Yadav S, Anbalagan M, Shi Y et al. Arsenic inhibits the adipogenic differentiation of mesenchymal stem cells by down-regulating peroxisome proliferator-activated receptor gamma and CCAAT enhancer-binding proteins. *Toxicol In Vitro*. 2013;27:211–219. doi: 10.1016/j.tiv.2012.10.012.
37. Zhao P, Deng Y, Gu P et al. Insulin-like growth factor 1 promotes the proliferation and adipogenesis of orbital adipose-derived stromal cells in thyroid-associated ophthalmopathy. *Exp Eye Res*. 2013;107:65–73. doi: 10.1016/j.exer.2012.11.014.
38. Galmozzi A, Mitro N, Ferrari A et al. Inhibition of class I histone deacetylases unveils a mitochondrial signature and enhances oxidative metabolism in skeletal muscle and adipose tissue. *Diabetes*. 2013;62:732–742. doi: 10.2337/db12-0548.
39. Jun Y, Xiao T, Guoyong Y et al. Recombinant globular adiponectin inhibits lipid deposition by p38 MAPK/ATF-2 and TOR/p70 S6 kinase pathways in chicken adipocytes. *Biochem Cell Biol*. 2014;92:53–60. doi: 10.1139/bcb-2013-0061.
40. Wakayama S, Haque A, Koide N et al. Lipopolysaccharide impairs insulin sensitivity via activation of phosphoinositide 3-kinase in adipocytes. *Immunopharmacol Immunotoxicol*. 2014;36:145–149. doi: 10.3109/08923973.2014.887096.

Submitted: 28 October, 2015
Accepted after reviews: 22 March, 2016
Available as AoP: 30 March, 2016